# Evaluation of Synthetic FK506 Analogues as Ligands for the FK506-Binding Proteins 51 and 52

Ranganath Gopalakrishnan,[†] Christian Kozany,[†] Steffen Gaali,[†] Christoph Kress,[†] Bastiaan Hoogeland,[†] Andreas Bracher,[‡] and Felix Hausch*[,†]

[†]Max Planck Institute of Psychiatry, Kraepelinstrasse 2, 80804 Munich, Germany
[‡]Max Planck Institute of Biochemistry, Am Klopferspitz 18, 82152 Martinsried, Germany

S *Supporting Information*

ABSTRACT: The FK506-binding proteins (FKBP) 51 and 52 are cochaperones that modulate the signal transduction of steroid hormone receptors. Both proteins have been implicated in prostate cancer. Furthermore, single nucleotide polymorphisms in the gene encoding FKBP51 have been associated with a variety of psychiatric disorders. Rapamycin and FK506 are two macrocyclic natural products that bind to these proteins indiscriminately but with nanomolar affinity. We here report the cocrystal structure of FKBP51 with a simplified *α*-ketoamide analogue derived from FK506 and the first structure−activity relationship analysis for FKBP51 and FKBP52 based on this compound. In particular, the *tert*-pentyl group of this ligand was systematically replaced by a cyclohexyl ring system, which more closely resembles the pyranose ring in the high-affinity ligands rapamycin and FK506. The interaction with FKBPs was found to be surprisingly tolerant to the stereochemistry of the attached cyclohexyl substituents. The molecular basis for this tolerance was elucidated by X-ray cocrystallography.
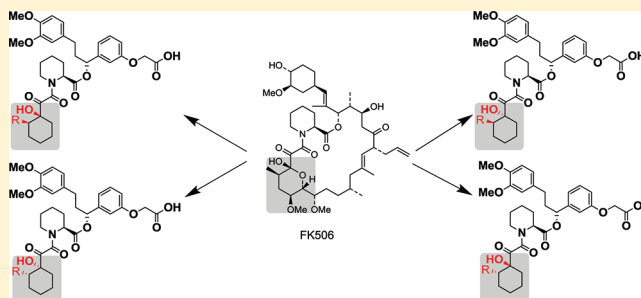
INTRODUCTION

Immunosuppressant natural products like FK506 (Figure 1a) and rapamycin bind with high affinity to immunophilins of the FKBP (FK506 binding protein) family, which often also possess peptidyl-propyl isomerase (PPIase) activity. The best-characterized member of the FKBP family is FKBP12, a 12 kDa protein, which consists only of the FK506-binding domain. FKBP12−FK506 and FKBP12−rapamycin complexes create binding surfaces for binding to calcineurin (CaN) and mTOR, respectively.[1] The inhibition of the latter proteins mediates the immunosuppressive action of the two natural products. FKBP12 has also been shown to modulate the ryanodine receptor (RyR) channels and to bind to the transforming growth factor *β* receptor I. FK506 inhibits these interactions consistent with a shared common binding site.[2]

The higher molecular weight FKBP homologues FKBP51 and FKBP52 act as cochaperones for the heat shock protein 90 (Hsp90). In the Hsp90 heterocomplex, FKBP51 and FKBP52 have been shown to modulate signal transduction by the glucocorticoid receptor in a mutually antagonistic direction.[3−5] FK506 was shown to inhibit the proliferation of prostate cancer cells. This was attributed to blockade of the enhancing effect of FKBP51 on the androgen receptor in these cells.[6,7] Numerous human genetic studies have shown that single nucleotide polymorphisms in the gene encoding FKBP51 are associated with a variety of psychiatric disorders.[8] Very recently, several independent studies using knockdown and knockout mice strongly supported an important role of FKBP51 in stress-

coping behavior.[9−12] These findings have rendered FKBP51 as a novel target for treatment of psychiatric disorders.[49] However, neither FK506 nor rapamycin can be used as a tool to investigate the roles of individual FKBPs in mammalian systems due to strong off-target effects and lack of selectivity. Thus, nonimmunosuppressive and selective inhibitors for the large FKBP homologues FKBP51 and FKBP52 are required.

At the end of the last millennium, various subclasses of high-affinity FKBP12 ligands were described, which were devoid of the immunosuppressive activity present in FK506 and rapamycin.[13,14] *α*-Ketoamide derivatives without the effector region were the most widely studied series exemplified by compound **2a**[15] (Figure 1). For FKBP12, the *tert*-pentyl group in **2a** was found to be a good surrogate for the pyranose group in FK506 and rapamycin.[16] While the high affinity of the natural products FK506 and rapamycin was retained for the larger FKBPs, the binding affinity of **2a** for the larger FKBPs was substantially weaker.[17] We thus first set out for a basic characterization of the structure−activity relationship of **2a**. To analyze the interactions with the 80s loop in more detail, we then substituted the *tert*-pentyl group in **2a** with cyclohexyl analogues, which more closely mimic the pyranose group in the high-affinity natural product ligands (Figure 1c).
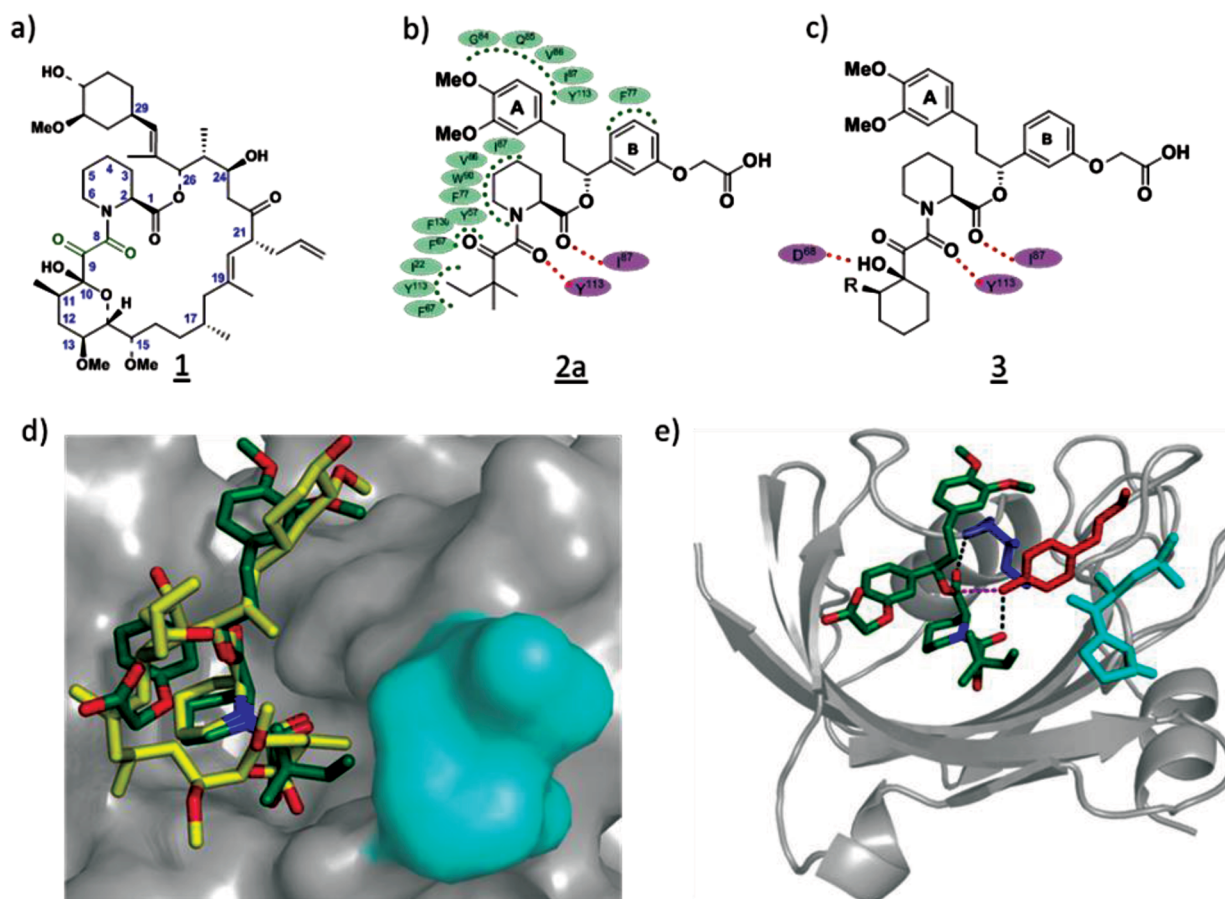
Figure 1. Natural and synthetic FKBP ligands: (a) Structure of FK506 (**1**), (b) prototypic synthetic ligand of FKBPs **2a**, which is devoid of immunosuppressive activity (hydrophobic contacts with FKBP51 are indicated in green, and hydrogen bonds are represented as pink dotted lines), (c) prototypic cyclohexyl-substituted ligand **3**, and (d and e) binding mode of **2a** with FKBP51. (d) Surface representation of FKBP51 in complex with **2a** (green). FK506 bound to FKBP51 (3O5R) is superimposed in yellow. (e) Ribbon representation of FKBP51 showing the conserved H-bonds between O[1]-**2a** and HN-Ile[87] (dark blue) and between O[8]-**2a** and HO-Tyr[113] (red) as black dotted lines. Leu[119] and Pro[120] at the top of the 80s loop are colored in cyan. The dipolar interaction between OH-Tyr[113] and C[1]-carbonyl is shown as a dotted line in magenta.

RESULT AND DISCUSSION

Crystal Structure of the 2a–FKBP51 Complex. As a structural starting point for a rational design the cocrystal structure of **2a**, the only synthetic ligand known for FKBP51, was solved in complex with the FK506-binding domain of FKBP51 at 1.5 Å resolution (Figure 1d,e). Upon binding of compound **2a**, FKBP51 adopts a very similar conformation as found in the FK506 complex[18] (Figure 1d). Most active site residues are virtually superimposable in the two cocrystal structures. As compared to the FK506 complex (3O5R), Phe[77] moves into the binding pocket, while Asp[68] and the tip of the 80s loop (Leu[119]-Lys[122]) move outward in the FKBP51–**2a** complex, the latter in part due to crystal contacts with a neighboring FKBP51 molecule.

The core interactions of FK506 are conserved for **2a** with the common pipecolate ring sitting atop the indole of Trp[90], which forms the floor of the FKBP binding pocket. The C[1]-carbonyl of the pipecolate forms a hydrogen bond with the backbone amide of Ile[87] (d = 2.92 Å), while the C[8]-carbonyl of the α-ketoamide engages in a hydrogen bond with the hydroxyl group of Tyr[113] (d = 2.65 Å). The latter approaches the C[1]-carbonyl at an angle of 107° and below van der Waals distance (3.17 Å), consistent with an attractive dipolar interaction.[19] The C[9]-keto oxygen of **2a** occupies a position similar to the keto group of FK506, while the hydrogen bond with Asp[68] seen in 3O5R is

no longer conserved because of the absence of the corresponding hydroxyl group in compound **2a**. The *tert*-pentyl group of compound **2a** sits in pocket formed by the 80s loop (Ser[118]-Ile[122]), which is occupied by the pyranose group of FK506 in the FK506–FKBP51 complex. As compared to a similar compound (SB3) in a complex with FKBP12 (1FKG[16]), the ethyl of the *tert*-pentyl group is rotated by 180° and faces the 80s loop. The dimethoxyaryl group (ring A) of **2a** sits in a cradle formed by residues Gly[84]-Ile[87] and Tyr[113] and engages in van der Waals contacts with Glu[20] from a neighboring FKBP51 molecule in the crystal. The acetyloxyaryl group (ring B) stacks on top of the edge of Phe[77], and its carboxyl moiety forms electrostatically enhanced hydrogen bonds with Lys[108] and Arg[31] from a neighboring molecule.

Structure–Activity Relationship (SAR) of the Pipecolate Core and Ester Substituent. So far, virtually nothing is known about the interaction of the large FKBPs with small molecule ligands. To the best of our knowledge, only one and three synthetic ligands have been described for FKBP51 and FKBP52, respectively.[17,20,21]

As a first characterization of the recognition properties of FKBP51 and FKBP52, we engaged on a basic SAR analysis of the prototypic ligand **2a**. The analogues of **2a** (Table 1) were synthesized by esterification or by alkylation of the C[1] carboxylate of the building blocks **4a–d** as outlined in Scheme

Table 1. FKBP Affinities of Synthetic FK506 Analogues

Compd. No	Structure	FKBP12	FKBP51FK1	FKBP52FK1
			IC$_{50}$(µM)^a	
2a		0.17 ± 0.05	8.36 ± 0.98	10.5 ± 1.5
2b		0.80 ± 0.05	51.5 ± 31.9	41.6 ± 15.8
2c		0.55 ± 0.06	32.73 ± 12.3	49.2 ± 24.6
2d		1.29 ± 0.14	>100	>100
2e		3.38 ± 0.54	>100	>100
6a		17.1 ± 2.7	>100	>100
6b	GPI-1046	1.24 ± 0.33	>100	>100
6c		2.11 ± 0.20	>150	>150
6d		2.45 ± 0.44	>100	>100
6e		0.10 ± 0.02	4.15 ± 1.45	2.8 ± 1.10
6f		1.05 ± 0.09	15.34 ± 1.94	5.55 ± 1.16
6g		0.10 ± 0.05	3.8 ± 1.05	1.07 ± 0.84
6h		0.15 ± 0.02	19.3 ± 6.6	11.6 ± 1.6
6i		0.017 ± 0.020	8.52 ± 2.81	7.37 ± 3.28
6j		>100	>100	>100

^{a}Binding affinities to FKBP12, FKBP51 (FK1 domain), and FKBP52 (FK1 domain) were determined by a fluorescence polarization assay.[17]

1 or Scheme S4 in the Supporting Information. The latter were prepared from the corresponding pipecolate analogues by N-oxalylation, introduction of the *tert*-pentyl moiety followed by deprotection of the C^1 carboxylate (Scheme S3 in the Supporting Information).[16] The 4,5-dehydropipecolate building block **4c** was synthesized from allyl glycine in four steps (Schemes S2 and S3 in the Supporting Information).[22] Building

block **5a** was obtained in 98% enantiomeric excess and 94% yield by a Noyori-catalyzed enantioselective reduction of the known keto precursor **13a** (Scheme S1 in the Supporting Information).[15] Building blocks **5b** (Scheme S1 in the Supporting Information) and **5c** were synthesized as described.[23]

In an initial SAR analysis, we explored the contributions of individual substructures in **2a** by first focusing on the pipecolate core. Replacement by a proline (**2b**) or a 4,5-dehydropipecolinic acid (**2c**) decreased the affinity for FKBPs 4−6-fold, while thiomorpholine-3-carboxylic acid (**2d**) abrogated detectable binding to the large FKBPs. Because even small changes at the core diminished affinity, we kept the pipecolate core constant in all further derivatives. We then replaced the pipecolate C^1 ester by an amide (**2e**), which completely abolished binding to larger FKBPs. This was anticipated since the additional hydrogen bond donor would point to the hydrophobic *tert*-pentyl group of **2e** when bound in a homologous binding mode as **2a**.

We next explored the requirements of the ester "top" group. Smaller substituents like in **6a−d** resulted in analogues with 7−100-fold lower affinity for FKBP12 and no activity for larger FKBPs as compared to **2a**. Compound **6b** (also called GPI-1046[24]) has been reported as one of the most potent and advanced inhibitors for FKBP12. Similar to the corresponding pipecolate analogue **6c**, GPI-1046 (**6b**) had no binding to larger FKBPs and micromolar affinity to FKBP12 in the fluorescence polarization assay, which is consistent with the discrepancies previously observed for GPI-1046 by others.[1] To eliminate the negative charge in **2a**, we exchanged the free acid moiety by a morpholine group (**6e**), which increased affinity 2−4-fold and induced a slight preference for FKBP52 vs FKBP51. A similar trend was also observed in a related sulfonamide pipecolate series.[48] In contrast to the carboxylic acid analogue **2b**, the morpholine-containing proline derivative **6f** retained detectable but 3-fold reduced binding. Replacement of the oxyacetyl group in **6g** by an amine resulted in a compound having similar affinity.

Finally, we replaced the *tert*-pentyl group with 3,4,5-trimethoxyphenyl in **6h** (Scheme S6 in the Supporting Information), which led to a 2-fold decrease in affinity for FKBP51, while having equivalent binding for FKBP12 and FKBP52. Additionally, two FK506 analogues that had been evaluated in the clinic were tested for their binding to the larger FKBPs.[1] Biricodar (VX-710, **6i**)[39] potently bound to FKBP12, while displaying moderate affinity for the larger FKBPs. In contrast, the related Timcodar (VX-853, **6j**), which lacks the pipecolate core, had no binding affinity for any FKBPs, consistent with the SAR data observed above.

Exploration of Pyranose/*tert*-Pentyl Analogues. A three-dimensional alignment of FKBP12- and the FK506-binding domains of FKBP51 and FKBP52 revealed that the core residues of the binding pockets are highly conserved. The largest differences were found in the adjacent 40s and 80s loops (residues 71−76 and 118−122 for FKBP51, respectively). The 80s loop of FKBP51 further contains Leu^{119}, which is replaced by Pro^{119} in FKBP52. Cellular studies have shown the residue at position 119 to be a major functional determinant for the effect on steroid hormone receptors.[25] Optimization of interactions with this part of the protein thus could impart selectivity and functional efficacy toward steroid hormone receptor for the large FKBPs. We therefore decided to investigate the interaction with this part of the protein in more detail.

Scheme 1. General Synthesis Protocol of Compounds 2a–d and 6a–h[a]

Scheme 2. General Synthesis Protocol of Diketo Acids 11a–e[a]
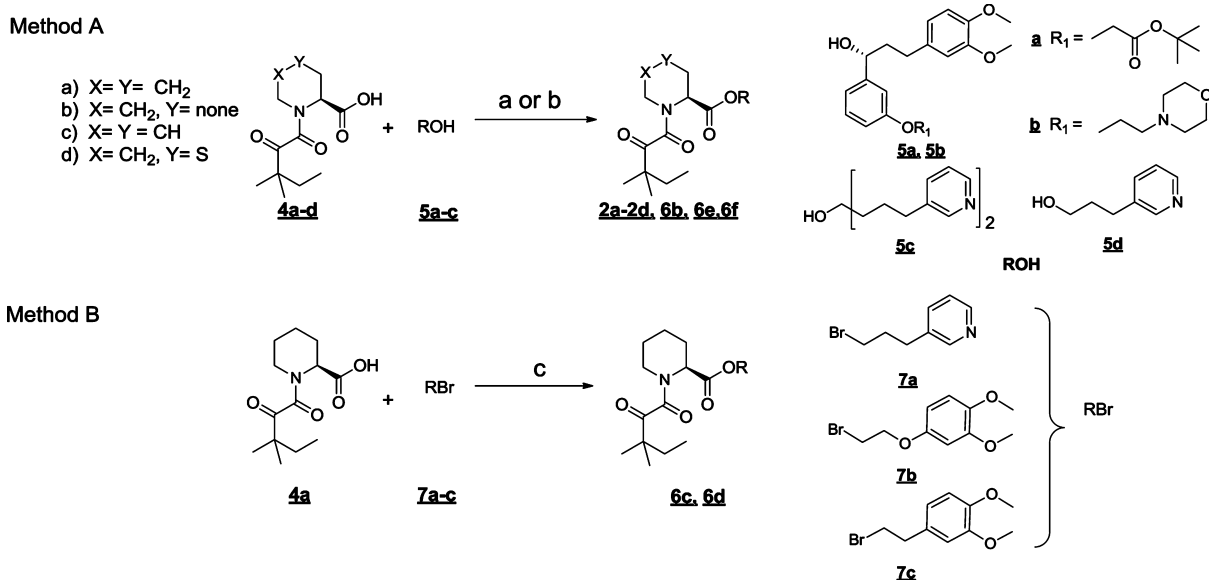
[a]Reagent and conditions: (a) DCC, DMAP, rt, 12h. (b) (i) DCC, DMAP, rt, 12h. (ii) 20% TFA in DCM, rt, 6 h, (c) DIPEA, toluene, reflux, 40 h.
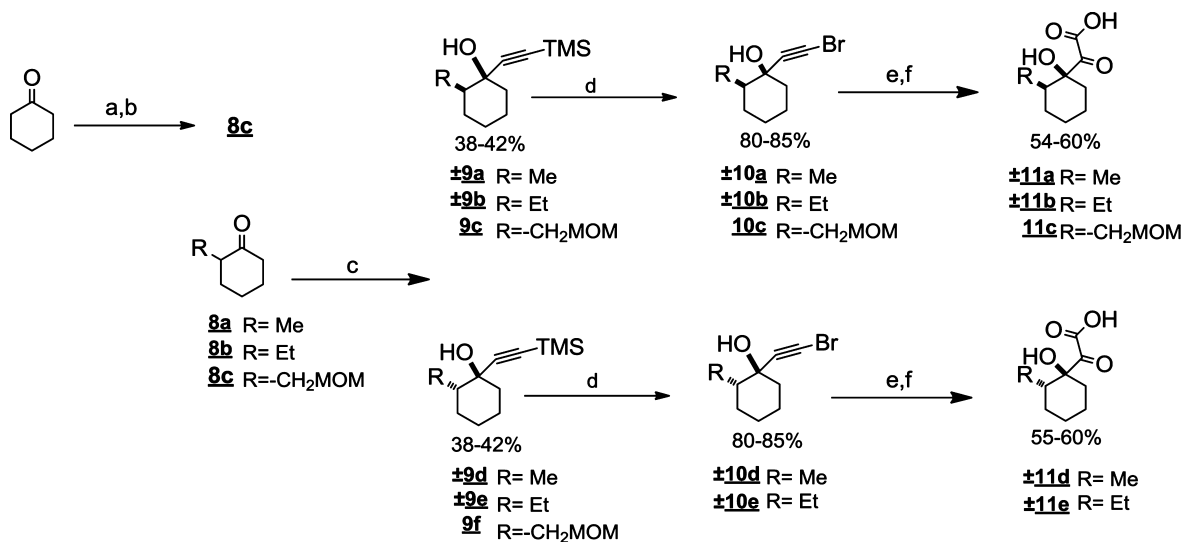
[a]Reagent and conditions: (a) L-Threonine, MgSO$_4$, HCHO, THF, 5 days. (b) MOMCl, DIPEA, DCM, 12 h. (c) TMS acetylene, n-BuLi, −78 °C, 2 h. (d) N-Bromosuccinimide, AgNO$_3$, acetone, 2 h. (e) KMnO$_4$, pH 7 (MgSO$_4$, NaHCO$_3$), MeOH:H$_2$O: 1:1, 0 °C to rt, 1 h. (f) 1 M LiOH, MeOH, 6 h.

The X-ray structure of FK506 with FKBP12 (1FKJ),[26] with the FK1 domains of FKBP51 (PDB code 3O5R)[18] and FKBP52 (manuscript in preparation) revealed that the pyranose group in FK506 (**1**) contacts the 80s loop. SAR studies around the pyranose group have shown that the methyl group at C[11] of FK506 analogues is important, while the pyranose ring oxygen is dispensable for binding to FKBP12.[27−29] This is consistent with the FK506-FKBP51 cocrystal structure where the C[11]-methyl fills a small hydrophobic cavity, while the pyranose ring oxygen of FK506 does not seem to act as a hydrogen bond acceptor.[18] The pyranose of FK506 further contains an exocyclic hydroxyl group at C[10] that engages in a hydrogen bond with Asp[68] of FKBP51. This could contribute to the higher affinity observed for the natural product. The **2a**–FKBP51 cocrystal structure shows that the

tert-pentyl group in **2a** occupies the same subpocket below the 80s loop as the pyranose ring in FK506. We therefore decided to replace the tert-pentyl group in **2a** with cyclohexyl derivatives that more closely resembled the pyranose in the high-affinity ligand FK506 (**1**). The first series of compounds investigated had a methyl substituent (**3a**) at C[11] as in FK506. The FK506–FKBP51 crystal structure (3O5R) further revealed that the 80s subpocket in the large FKBPs is more open and has a potential hydrogen bond interaction partner (S[118]) in its vicinity. We therefore also prepared cyclohexyl analogues with larger or hydrophilic C[11] substituents.

A four-step synthesis scheme for the α-keto acids **11a,b** and **11d,e** was set up starting from the corresponding racemic cyclohexanones **8a** or **8b** (Scheme 2). Alternatively, for **11c**, the enantiopure MOM-protected 2-hydroxymethyl cyclohexanone

Scheme 3. General Synthesis Protocol of Compounds 3a–j[a]
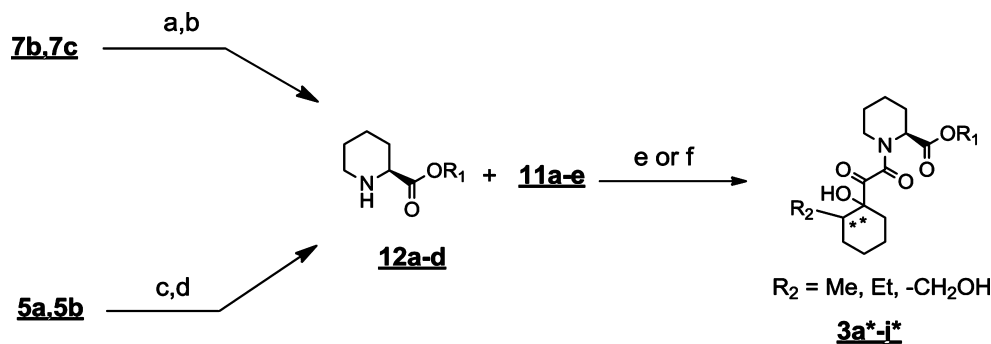
aReagent and conditions: (a) (S)-1-Boc-piperidine-2-carboxylic acid, K_2CO_3, KI, 60 °C, 12 h. (b) 20% TFA in DCM, rt, 2 h. (c) (S)-1-Fmoc-piperidine-2-carboxylic acid, DCC, DMAP, rt, 12 h. (d) 20% 4-methylpiperidine in DCM, rt, 4h. (e) Compounds **11a–e**, HATU, DIPEA, rt, 16 h. (f) (i) Compounds **11a–e**, HATU, DIPEA, rt, 16 h; (ii) 20% TFA in DCM, rt, 6 h.

8c was used. The latter was obtained in two steps from cyclohexanone by an organocatalyzed formylation.[30,31] TMS acetylene was reacted with **8a–c** to obtain the cis and trans diastereomers **9a–f**[32] (stereochemistry assigned by NMR[33]) in nearly equal amounts, which could be separated using column chromatography. N-Bromosuccinimide was used to cleave the TMS group and introduce the bromide at the terminal alkynes (**10a–e**)[34] followed by oxidation of the activated alkynes by $KMnO_4$ to yield the corresponding α-keto esters.[35−38] These were further hydrolyzed to give the α-keto acids **11a,b** and **11d,e**, as racemic mixtures, and enantiopure **11c**.

The α-keto acids (**11a–e**) were coupled with the pipecolic acid building blocks **12a–d** as outlined in Scheme 3 to give compounds **3a–g** and **3i,j** as mixture of diastereomers and **3h** as a single pure diastereomer. The affinities for FKBPs were either tested as mixture of diastereomers (**3a–g** and **3i,j**) or after diastereomeric separation using preparative HPLC (Table 2).

Introduction of the FK506-like cyclohexyl moiety in **3a** increased affinity for FKBPs 2-fold as compared to **2a**, indicating that the cyclohexyl moiety might indeed better interact with the 80s loop than the *tert*-pentyl group. We next explored the influence of the ester "top" group in the context of the cyclohexyl substituent. Removing the acetyloxyaryl ring (ring B) as in **3c** reduced the affinity for FKBPs by 6-fold. This is in contrast to the results observed for the C^{11}-ethyl analogue **3d** and the corresponding *tert*-pentyl containing substance **6d**. Further shortening of the linker connecting the dimethoxyaryl moiety (ring A) as in **3b** substantially decreased affinity for all FKBPs. This indicates that the linker length is critical for optimal positioning of the dimethoxyaryl moiety, at least in the cyclohexyl series. Similar to the *tert*-pentyl series, replacement of the carboxylate by a morpholine in compounds **3e** and **3g** increased affinity for FKBPs and induced a slight preference for FKBP52 as compared to FKBP51.

We next investigated the role of the C^{11} substituent on the cyclohexyl moiety. The C^{11}-methyl (**3a***), C^{11}-ethyl (**3f***), and C^{11}-hydroxylmethyl derivative (**3h**) had similar binding for the larger FKBPs, while the affinity for FKBP12 was reduced. Importantly, however, we also found that the diastereomeric mixtures **3i*** and **3j*** had almost equivalent binding to FKBPs as their FK506-like counterparts **3a*** and **3f***. This was somewhat surprising since in the "unnatural" diastereomers **3i*** and **3j***, the Asp^{68}-HO^{10} hydrogen bond and hydrophobic 80s loop contacts of the C^{11} substituent are not possible at the same

time. To further investigate the influence of stereochemistry and the substitution pattern at the cyclohexyl ring in more detail, we separated the individual diastereomers **3a-1**, **3a-2**, **3i-1**, **3i-2**, **3f-1**, and **3f-2**.

Again, these diastereomers had almost equivalent binding to the proteins. These observations led us to conclude that in linear FK506 analogues the stereochemistry around the pyranose group per se is not as important for activity as previously thought and that the 80s loop is flexible enough to accommodate the small stereo chemical changes in the active site.

Cocrystal Structures of 3f-1 and 3f-2. To understand the unexpected binding of the noncanonical diastereomers, we solved the cocrystal structure of both **3f-1** and **3f-2** with the FK506-binding domain of FKBP51 (Figure 2). Depending on whether the complexes were crystallized or the compounds were added to preformed crystals, different crystal forms were obtained. In both cocrystal lattices, the ligands engaged Glu^{20}, Arg^{31}, and Lys^{108} of a neighboring FKBP51 molecule, similar to the crystal contacts observed for **2a** (see above).

Upon binding of compound **3f-1** or **3f-2**, FKBP51 adopts the same structure as found in FKBP51 complexed with **1** and **2a**. Likewise, the binding modes for the pipecolate, the ester "top" group, and the α-keto amide of **3f-1** or **3f-2** were almost perfectly superimposable to those found for **2a** in complex with FKBP51. In particular, the hydrogen bond network and the dipolar interaction comprising Ile^{87}-NH, C^1=O, Tyr^{113}-OH, and C^8=O are conserved. In **3f-1**, a hydrogen bond of C^{10}-OH with Asp^{68} (d = 2.75 Å) is formed similar to the one observed for the pyranose group of FK506 (PDB code 3O5R). However, the cyclohexyl group in **3f-1** is slightly lifted out of the binding pocket and slightly rotated likely to relieve a steric clash of the larger C^{11} substituent. For the C^{11} substituent, two orientations seem to be possible, which occupy similar positions like the ethyl group of the *tert*-pentyl moiety in **2a** (Figure 2a). In the case of **3f-2**, the cyclohexyl moiety is rotated by 180°, which allows the C^{11} ethyl substituent to occupy almost an identical position as for **3f-1**, indicating that this hydrophobic interaction might be rather important (Figure 2b). In this conformation, the hydrogen bond with Asp^{68} is no longer possible, but the C^{10}-OH now forms water-mediated hydrogen bonds to Tyr^{113} and Ser^{118}. This water network might provide the binding energy to compensate for the loss of the C^{10}-OH···Asp^{68} H-bond.

Table 2. FKBP affinities of Pyranose Analogs

Compd. No.	R1	FKBP12	FKBP51FK1	FKBP52FK1
			$IC_{50}(\mu M)^a$	
3a*		0.06 ± 0.004	4.20 ± 0.11	2.13 ± 0.21
3b*		2.2 ± 0.5	>100	>100
3c*		0.31 ± 0.04	29.39 ± 8.5	11.7 ± 6.4
3d*		2.78 ± 0.02	>100	>100
3e*		0.06 ± 0.004	2.02 ± 0.14	0.89 ± 0.06
3f*		0.32 ± 0.025	3.9 ± 1.2	9.5 ± 1.3
3f-1		0.13 ± 0.03	5.8 ± 0.6	4.2 ± 0.3
3f-2		0.343 ± 0.09	3.9 ± 0.6	3.5 ± 0.6
3g*		0.47 ± 0.06	9.66 ± 0.83	3.72 ± 1.02
3h		0.51 ± 0.08	8.5 ± 0.6	6.2 ± 0.5
3i*		0.06 ± 0.004	4.13 ± 0.20	2.64 ± 0.19
3a-1		0.06 ± 0.004	4.27 ± 0.19	2.44 ± 0.17
3a-2		0.05 ± 0.006	4.54 ± 0.24	2.88 ± 0.21
3i-1		0.05 ± 0.005	4.18 ± 0.15	2.20 ± 0.13
3i-2		0.06 ± 0.003	4.96 ± 0.25	2.64 ± 0.25
3j*		0.57 ± 0.12	9.13 ± 0.59	9.77 ± 1.48

[a]Binding affinities to FKBP12, FKBP51 (FK1 domain), and FKBP52 (FK1 domain) were determined by a fluorescence polarization assay.[17]
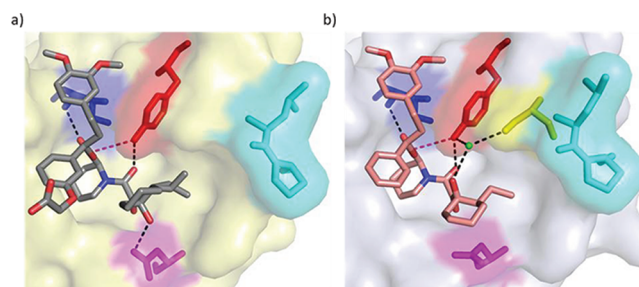

Figure 2. X-ray crystal structure of **3f-1** and **3f-2** in the FK506-binding domain of FKBP51. The hydrogen bonds between O^1 and HN-Ile[87] (shadowed blue) and between O^8 and HO-Tyr[113] (shadowed red) are represented as dotted black lines. The dipolar interaction between OH-Tyr[113] and C^1 carbonyl is indicated by a dotted pink line. Leu[119] and Pro[120] of the 80s loop are indicated in cyan. (a) Binding mode of **3f-1** in the active site of FKBP51. The additional hydrogen bond between HO[10]-**3f-1** and O-Asp[68] (shadowed magenta) is shown as dotted black line. (b) Binding mode of **3f-2** in the active site of FKBP51. The hydrogen bond network formed by a water molecule (green) with Tyr[113] and Ser[118] (yellow) of FKBP51 and with C^{10}-OH of **3f-2** complex is indicated by a dotted black line.

■ CONCLUSION

This study for the first time describes a detailed SAR of ligands for the larger FKBPs 51 and 52. Although SAR of α-ketoamides for FKBP12 has been extensively documented, this is the first instance where a direct comparison of binding trends between FKBP12 and larger FKBPs have been studied. The X-ray cocrystal structure of **2a** was obtained as the starting point, followed by a systematic exploration of the contributions of each substituent on affinity to FKBP51 or FKBP52. Larger top groups as in **2a** and **6e** were found to have better binding affinity, while the pipecolic core (**2a**) was found to be essential. The *tert*-pentyl group in **2a** was further substituted by a cyclohexyl group, which mimicked the pyranose in FK506 and rapamycin. From the binding studies and X-ray cocrystal structure of the diastereomers (**3f-1** and **3f-2**), we can conclude that the FKBPs are tolerant toward change of the stereochemistry around the cyclohexyl (pyranose) substituents, at least in a linear, unconstrained context. These cocrystal structures also suggest that multiple molecular binding modes are possible for the 80s loop interaction, which is in line with the high flexibility of this region.

■ EXPERIMENTAL SECTION

Chemistry. Chromatographic separations were performed either by manual flash chromatography or by automated flash chromatography using an Interchim Puriflash 430 with an UV detector. Organic phases were dried over $MgSO_4$, and the solvents were removed under reduced pressure. Merck F-254 (thickness 0.25 mm) commercial plates were used for analytical TLC to follow the progress of reactions. Silica gel 60 (Merck 70–230 mesh) was used for manual column chromatography. Unless otherwise specified, ^{1}H NMR spectra, ^{13}C NMR spectra, 2D HSQC, HMBC, and COSY of all intermediates were obtained from the Department of Chemistry and Pharmacy, LMU, on a Bruker AC 300, a Bruker XL 400, or a Bruker AMX 600 at room temperature. Chemical shifts for ^{1}H or ^{13}C are given in ppm (δ) relative to tetramethylsilane (TMS) as an internal standard. Mass spectra (m/z) were recorded on a Thermo Finnigan LCQ DECA XP Plus mass spectrometer at the Max Planck Institute of Psychiatry, while the high-resolution mass spectrometry was carried out at MPI for Biochemistry (Microchemistry Core facility) on Varian Mat711 mass spectrometer. The purity of the compounds was verified by reversed phase HPLC. All of the final compounds synthesized and

tested have a purity of more than 95%. The optical rotation for the compounds was obtained from the Department of Chemistry and Pharmacy, LMU, on a Perkin-Elmer 241 polarimeter.

HPLC Conditions for Product Analysis. Column: Jupiter 4 μm Proteo 90 A, 250 mm × 4.6 mm, Phenomenex, Torrance, CA; wavelength: 224 nm, 280 nm; flow rate: 1 mL/min; buffer A: 0.1% TFA in 5% MeCN/water; buffer B: 0.1% TFA in 95% MeCN/water. Gradient A: after 1 min elution with 100% buffer A, linear gradient of 0−100% buffer B for 30 min.

LCMS Conditions for Product Analysis. Column: YMC Pack Pro C8, 100 mm × 4.6 mm, 3 μm; wavelength: 224 nm, 280 nm; flow rate: 1 mL/min; buffer A: 0.1% HCOOH in 5% MeCN/water; buffer B: 0.1% HCOOH in 95% MeCN/water. Gradient A: 1 min 100% buffer A, then linear gradient of 0−100% buffer B for 11 min.

Preparative HPLC for Diasteromer Separation. The compounds were dissolved in 40% buffer B, and the purification was carried out with a injection loop volume of 2 mL. Column: Jupiter 10 μm Proteo 90 A, 250 mm × 21.7 mm, 10 μm, Phenomenex; wavelength: 224 nm; flow rate: 25 mL/min; buffer A: 0.1% TFA in 5% MeOH/water; buffer B: 0.1% TFA in 95% MeOH/water.

Synthesis of (S)-Methyl 1-(3,3-Dimethyl-2-oxopentanoyl)-piperidine-2-carboxylate (4a). The compound was prepared as described previously.[16]

Synthesis of (S)-Methyl 1-(3,3-Dimethyl-2-oxopentanoyl)-pyrrolidine-2-carboxylate (4b). The compound was prepared from the methyl ester of L-proline in an analogous manner to **4a**.

General Method A. A solution of alcohol **5a−c**, carboxylic acid **4a−d**, and DMAP in DCM at room temperature was treated with DCC. After it was stirred for 12 h, the mixture was diluted with EtOAc and filtered through a plug of Celite. The filtrate was concentrated, and the crude material was flash chromatographed to afford the product.

General Method B. A solution of bromide **7a−c** and carboxylic acid **4a** or **4b** was treated with DIPEA in toluene at reflux for 40 h. Afterwards, the mixture was diluted with EtOAc (30 mL) and filtered through a plug of Celite. The filtrate was concentrated, and the crude material was flash chromatographed to afford the product.

Synthesis of 2-(3-((R)-3-(3,4-Dimethoxyphenyl)-1-((S)-1-(3,3-di-methyl-2-oxopentanoyl)piperidine-2-carbonyloxy)propyl)phenoxy)-acetic Acid (2a). The compound was prepared as described previously.[17]

General Procedure for the Synthesis of 2-Alkyl-1-((trimethylsilyl)-ethynyl)cyclohexanol (9). The THF solution of the lithium reagent was generated by treating trimethylsilylacetylene (3 mL, 21.4 mmol) with n-BuLi (2 M in hexane, 11.6 mL) at −78 °C. The solution was stirred for 0.5 h at that temperature. To this, a solution of 2-alkylcyclohexanone (**8a−c**) (17.8 mmol) in THF (5 mL) was added and stirred for an additional 2 h. Then, the solution was quenched by addition of a saturated aqueous NH$_4$Cl solution. The organic phase was separated, and the aqueous phase was extracted with ethyl acetate (3 × 100 mL). The combined organic phases were washed with brine (30 mL) and dried over MgSO$_4$. The solution was concentrated and then flash chromatographed using hexane:EtOAc 9:1 to afford each of the two diastereomers **9a−f**.

(1S,2R)-2-Methyl-1-((trimethylsilyl)ethynyl)cyclohexanol and (1R,2S)-2-Methyl-1-((trimethylsilyl)ethynyl)cyclohexanol (9a). Compound **9a** (1.2 g, 33%) was obtained from **8a** (2 g) as a colorless liquid. TLC (hexane:EtOAc 9:1): R_f = 0.36. ^{1}H NMR (300 MHz, CDCl$_3$) δ = 0.17 (s, 9H), 1.06 (d, 3H, J = 6.9 Hz), 1.23−1.33 (m, 1H), 1.48−1.71 (m, 7p), 1.95−2.02 (m, 1P). ^{13}C NMR (75 MHz, CDCl$_3$) δ = 0.01, 16.00, 21.06, 25.02, 29.15, 39.15, 40.48, 69.77, 86.95, 110.61. HRMS: 193.1390 [M − OH]$^+$; calculated, 193.1413 [M − OH]$^+$.

(1S,2R)-2-Ethyl-1-((trimethylsilyl)ethynyl)cyclohexanol and (1R,2S)-2-Ethyl-1-((trimethyl silyl)ethynyl)cyclohexanol (9b). Compound **9b** (1.65 g, 46%) was obtained from **8b** (2.2 g) as a colorless liquid. TLC (hexane:EtOAc 9:1): R_f = 0.40. ^{1}H NMR (300 MHz, CDCl$_3$) δ = 0.17 (s, 9H), 0.86−0.96 (m, 6H), 1.12−2.42 (m, 22H). ^{13}C NMR (75 MHz, CDCl$_3$) δ = 0.024, 11.68, 12.30, 21.23, 22.88, 24.80, 25.46, 28.00, 33.28, 39.47, 41.94, 47.47, 52.31, 70.32, 87.09, 110.85. HRMS: 208.2069 [M − OH]$^+$; calculated, 208.1569 [M − OH]$^+$.

General Procedure for the Synthesis of 2-Alkyl-1-(bromoethynyl)-cyclohexanol (10). To a solution of **9a−e** (1.3 mmol), N-bromosuccinimide (1.5 mmol) and AgNO$_3$ (0.5 mmol) in acetone (10 mL) were added, and the resulting solution was stirred in darkness for 2 h at room temperature. Acetone was evaporated under reduced pressure, and the solids were removed by filtration through a Celite pad (washing with ether). The combined organic phase were concentrated and subjected to purification by column chromatography using hexane:EtOAc 9:1 to yield **10a−e** as yellow liquids.

(1S,2R)-1-(Bromoethynyl)-2-methylcyclohexanol and (1R,2S)-1-(Bromoethynyl)-2-methylcyclohexanol (10a). Compound **10a** (256 mg, 91%) was obtained from **9a** (273 mg) as a yellow liquid. TLC (hexane:EtOAc 9:1): R_f = 0.30. ^{1}H NMR (300 MHz, CDCl$_3$) δ = 1.06 (d, 3H, J = 6.9 Hz), 1.29−1.73 (m, 8H), 1.97−2.04 (m, 1H). ^{13}C NMR (75 MHz, CDCl$_3$) δ = 16.05, 20.94, 24.95, 29.09, 39.17, 40.52, 43.04, 70.79, 84.60. HRMS: m/z 199.0193, 201.0169 [M − OH]$^+$; calculated, 199.0122, 201.0102 [M − OH]$^+$.

(1S,2R)-1-(Bromoethynyl)-2-ethylcyclohexanol and (1R,2S)-1-(Bromoethynyl)-2-ethylcyclohexanol (10b). Compound **10b** (264 mg, 88%) was obtained from **9b** (292 mg) as a yellow liquid. TLC (hexane:EtOAc 9:1): R_f = 0.36. ^{1}H NMR (300 MHz, CDCl$_3$) δ = 0.96 (d, 3H, J = 7.2 Hz), 1.13−1.30 (m, 3H), 1.36−1.45 (m, 1H), 1.50−1.74 (m, 5H), 1.83−2.02 (m, 2H). ^{13}C NMR (75 MHz, CDCl$_3$) δ = 12.17, 21.10, 23.03, 24.81, 25.35, 39.55, 43.17, 47.78, 71.39, 84.74. HRMS: m/z 213.0268, 215.0245 [M − OH]$^+$; calculated, 213.0279, 215.0259 [M − OH]$^+$.

General Procedure for the Synthesis of 2-(1-Hydroxy-2-alkylcyclohexyl)-2-oxoacetic Acid (11a−e). To the above synthesized α-ketoesters was added 1 M LiOH in MeOH:H$_2$O (1:1), and the reaction was stirred for 6 h at room temperature. The reaction was acidified to pH 2 by the addition of 1 M HCl. The aqueous layer was extracted with ethyl acetate (3 × 20 mL). The combined organic phases were washed with brine (30 mL) and dried over MgSO$_4$. The solution was concentrated under reduced pressure to furnish the free acid **11a−e** as an oily liquid.

2-((1S,2R)-1-Hydroxy-2-methylcyclohexyl)-2-oxoacetic Acid and 2-((1R,2S)-1-Hydroxy-2-methylcyclohexyl)-2-oxoacetic Acid (11a). Compound **11a** (105 mg, overall yield for two steps 52%) was obtained from **10a** (235 mg) as a oily liquid. TLC (hexane:EtOAc:T-FA 9:1:0.1): R_f = 0.28. ^{1}H NMR (400 MHz, CDCl$_3$) δ = 0.78 (d, 3H, J = 6.8 Hz), 1.33−1.95 (m, 8H), 2.15−2.24 (m, 1H). ^{13}C NMR (100 MHz, CDCl$_3$) δ = 16.32, 20.32, 25.46, 29.41, 35.12, 36.57, 81.55, 162.81, 200.53.

2-((1S,2R)-2-Ethyl-1-hydroxycyclohexyl)-2-oxoacetic Acid and 2-((1R,2S)-2-Ethyl-1-hydroxycyclohexyl)-2-oxoacetic Acid (11b). Compound **11b** (141 mg, overall yield for two steps 65%) was obtained from **10b** (250 mg) as a oily liquid. TLC (hexane:EtOAc:TFA 9:1:0.1): R_f = 0.26. ^{1}H NMR (400 MHz, CDCl$_3$) δ = 0.83 (t, 3H, J = 7.6 Hz), 1.13−1.36 (m, 4H), 1.57−1.62 (m, 2H), 1.73−1.96 (m, 5H). ^{13}C NMR (100 MHz, CDCl$_3$) δ = 11.82, 20.39, 23.95, 25.08, 25.46, 35.32, 43.14, 82.20, 164.12, 201.23.

General Procedure for Coupling of 12a−d with 11a−e To Yield 3a−3j*.* To a stirred solution of the free amines (**12a−d**) in acetonitrile under argon was added sequentially N,N-diisopropyl-ethylamine (DIPEA), HATU, and the diketoacids (**11a−e**). The reaction mixture was stirred for 16 h at room temperature. Saturated NH$_4$Cl solution was added to the reaction, and the solution was stirred for 10 min. The organic phase was separated, and the aqueous phase was extracted with ethyl acetate (3 × 100 mL). The combined organic phases were washed with brine (10 mL) and dried over MgSO$_4$, and the residual solid was purified by column chromatograpahy.

Synthesis of 2-(3-((R)-3-(3,4-Dimethoxyphenyl)-1-((S)-1-(2-((1S,2R)-1-hydroxy-2-methylcyclohexyl)-2-oxoacetyl)piperidine-2-carbonyloxy)propyl)phenoxy)acetic Acid and 2-(3-((R)-3-(3,4-Dime-thoxyphenyl)-1-((S)-1-(2-((1R,2S)-1-hydroxy-2-methylcyclohexyl)-2-oxoacetyl)piperidine-2-carbonyloxy)propyl)phenoxy)acetic Acid (3a).* Compound **3a*** ester (46 mg, 0.067 mmol) was treated with 20% TFA in DCM at room temperature. The mixture was allowed to stir for 6 h. TFA and DCM were evaporated under reduced pressure to yield the free acid **3a*** (32 mg, 0.051 mmol, 77%).

TLC (hexane:EtOAc:TFA 6:3.9: 0.1): R_f = 0.33. HPLC (gradient A) retention time = 24.6−25.1 min. ^{1}H NMR (600 MHz, CDCl$_3$) δ = 0.82−0.88 (m, 3H), 1.36−1.92 (m, 13H), 2.03−2.13 (m, 2H), 2.23−2.38 (m, 2H), 2.50−2.67 (m, 2H), 3.24−3.31 (m, 1H), 3.48−3.55 (m, 1H), 3.85 (s, 3H), 3.86 (s, 3H), 4.67 (s, 2H), 5.25−5.27 (m, 2H), 5.74−5.77 (m, 1H), 6.56−6.70 (m, 2H), 6.77−6.80 (m, 1H), 6.82−6.87 (m, 1H), 6.89−6.96 (m, 2H), 7.26−7.29 (m, 1H). ^{13}C NMR (150 MHz, CDCl$_3$) δ = 16.3, 20.16, 20.87, 24.79, 25.29, 26.55, 29.30, 31.35, 35.59, 37.60, 39.45, 44.28, 51.92, 55.87, 55.92, 65.07, 76.86, 82.24, 111.37, 111.70, 115.71, 116.21, 119.71, 120.20, 129.90, 133.21, 141.51, 147.41, 148.89, 157.74, 167.39, 169.20, 171.63, 205.23. MS (ESI) m/z: found R_t 13.88 min. Method LCMS, 648.45 [M + Na]$^+$. HRMS: 626.2902 [M + H]$^+$; calculated, 626.2887 [M + H]$^+$. The diasteromeric mixture was further separated using preparative HPLC gradient 62−77% B for 35 min to yield diasteromer **3a-1** (6 mg) and **3a-2** (9 mg).

3a-1. HPLC (gradient A) retention time = 24.6−24.8 min. ^{1}H NMR (600 MHz, CDCl$_3$) δ = 0.82 (d, 3H, J = 5.4 Hz), 1.38−1.43 (m, 2H), 1.44−1.48 (m, 2H), 1.53−1.58 (m, 2H), 1.64−1.70 (m, 3H), 1.74−1.81 (m, 2H), 2.04−2.12 (m, 2H), 2.22−2.28 (m, 1H), 2.52−2.67 (m, 2H), 2.98 (d, 1 h, J = 5.4 Hz), 3.08 (s, 1H), 3.12 (s, 1H), 3.25 (dt, 1H, J = 2.4, 13.2 Hz), 3.53 (d, 1H, J = 13.2 Hz), 3.64−3.67 (m, 1H), 3.72 (s, 1H), 3.85 (s, 3H), 3.86 (s, 3H), 4.63 (s, 2H), 5.24 (d, 1H, J = 4.8 Hz), 5.74−5.80 (m, 1H), 6.66−6.69 (m, 2H), 6.77−6.79 (m, 1H), 6.83−6.94 (m, 3H), 7.26−7.28 (m, 1H). ^{13}C NMR (150 MHz, CDCl$_3$) δ = 16.15, 20.18, 21.06, 24.79, 25.27, 26.52, 29.68, 31.41, 35.57, 36.61, 37.64, 44.18, 51.88, 55.86, 55.92, 63.81, 81,38, 111.35, 111.68, 115.65, 115.66, 119.54, 120.16, 129.85, 133.19, 141.53, 147.45, 148.93, 157.92, 167.57, 169.26, 169.26, 205.46. MS (ESI) m/z: found R_t 13.87 min. Method LCMS, 648.40 [M + Na]$^+$; calculated, 648.45 [M + Na]$^+$. $^{21}\alpha_D$ = −2.62°.

3a-2. HPLC (gradient A) retention time = 24.9−25.1 min. ^{1}H NMR (600 MHz, CDCl$_3$) δ = 0.84 (d, 3H, J = 6.6 Hz), 1.38−1.85 (m, 10H), 2.06 (s, 2H), 2.20−2.31 (m, 1H), 2.49−2.65 (m, 2H), 2.97 (d, 1H, J = 6.6 Hz), 3.05 (s, 1H), 3.12 (s, 1H), 3.25 (t, 1H, J = 12.6 Hz), 3.48 (d, 1H, J = 10.8 Hz), 3.65 (s, 1H), 3.72 (s, 2H), 3.84 (s, 3H), 3.85 (s, 3H), 4.81 (s, 1H), 5.26 (s, 1H), 5.74 (s, 1H), 6.66−6.68 (m, 2H), 6.77−6.94 (m, 4H), 7.21−7.24 (m, 1H). ^{13}C NMR (150 MHz, CDCl$_3$) δ = 16.15, 20.21, 20.94, 24.82, 25.31, 26.40, 29.68, 31.35, 35.31, 36.72, 37.15, 42.16, 43.25, 44.25, 44.54, 46.53, 48.81, 51.75, 55.86, 55.92, 56.79, 63.84, 81.66, 111.34, 111.70, 115.51, 119.59, 120.17, 129.82, 133.32, 141.58, 147.41, 148.91, 157.91, 167.37, 169.34, 205.95. MS (ESI) m/z: found R_t 13.91 min. Method LCMS, 648.31 [M + Na]$^+$; calculated, 648.45 [M + Na]$^+$. $^{21}\alpha_D$ = +0.31°.

Synthesis of 2-(3-((R)-3-(3,4-Dimethoxyphenyl)-1-((S)-1-(2-((1S,2R)-2-ethyl-1-hydroxycyclohexyl)-2-oxoacetyl)piperidine-2-carbonyloxy)propyl)phenoxy)acetic Acid and 2-(3-((R)-3-(3,4-Dimethoxyphenyl)-1-((S)-1-(2-((1R,2S)-2-ethyl-1-hydroxycyclohexyl)-2-oxoacetyl)piperidine-2-carbonyloxy)propyl)phenoxy)acetic Acid (3f*). Compound **3f*** ester (62 mg, 0.089 mmol) was treated with 20% TFA in DCM at room temperature. The mixture was allowed to stir for 6 h. TFA and DCM were evaporated under reduced pressure to yield the free acid **3f*** (40 mg, 0.062 mmol, 80%).

TLC (hexane:EtOAc:TFA 1:1:0.2): R_f = 0.45. HPLC (gradient A) retention time = 25.3−25.9 min. MS (ESI) m/z: found R_t 15.93 min. Method LCMS, 662.63 [M + Na]$^+$. HRMS: 640.3739 [M + H]$^+$; calculated, 640.3043 [M + H]$^+$. The diasteromeric mixture was further separated using preparative HPLC gradient 65−70% B for 15 min to yield diasteromer **3f-1** (5 mg) and **3f-2** (7 mg).

3f-1. HPLC (gradient A) retention time = 25.3−25.5 min. HRMS: 640.3773 [M + H]$^+$; calculated, 640.3043 [M + H]$^+$.

3f-2. HPLC (gradient A) retention time = 25.7−25.9 min. HRMS: 640.3764 [M + H]$^+$; calculated, 640.3043 [M + H]$^+$.

Crystallography. Crystals and cocrystals of the FKBP51 Fk1 domain construct comprising residues 16−140 and containing mutation A19T were obtained as previously described.[18] Diffraction data were collected at the European Synchrotron Radiation Facility (ESRF) in Grenoble, France. The data were processed with MOSFLM[40] and XDS,[41] SCALA,[42] and TRUNCATE.[43] The crystal structures were solved by molecular replacement employing the program MOLREP.[44] The dictionaries for the ligand compounds were generated with the PRODRG server.[45] The structures were refined with REFMAC.[46] Manual model building was performed with COOT.[47] Molecular graphics figures were generated using PyMOL (http://www.pymol.org).

ASSOCIATED CONTENT

Ⓢ Supporting Information

Reaction schemes and spectroscopic details of intermediates. This material is available free of charge via the Internet at http://pubs.acs.org.

AUTHOR INFORMATION

Corresponding Author

*Tel: +49(89)30622640. Fax: +49(89)30622610. E-mail: hausch@mpipsykl.mpg.de.

Notes

The authors declare no competing financial interest.

ABBREVIATIONS USED

FKBP, FK506 binding protein; Hsp90, heat shock protein 90; SAR, structure−activity relationship

REFERENCES

(1) Gaali, S.; Gopalakrishnan, R.; Wang, Y.; Kozany, C.; Hausch, F. The Chemical Biology of Immunophilin Ligands. *Curr. Med. Chem.* **2011**, *18*, 5355−5379.

(2) Huse, M.; Chen, Y.-G.; Massague, J.; Kuriyan, J. Crystal Structure of the Cytoplasmic Domain of the Type I TGF [beta] Receptor in Complex with FKBP12. *Cell* 1999, *96*, 425−436.

(3) Riggs, D. L.; Roberts, P. J.; Chirillo, S. C.; Cheung-Flynn, J.; Prapapanich, V.; et al. The Hsp90-binding peptidylprolyl isomerase FKBP52 potentiates glucocorticoid signaling in vivo. *EMBO J.* 2003, *22*, 1158−1167.

(4) Wochnik, G. M.; Ruegg, J.; Abel, G. A.; Schmidt, U.; Holsboer, F.; et al. FK506-binding Proteins 51 and 52 Differentially Regulate Dynein Interaction and Nuclear Translocation of the Glucocorticoid Receptor in Mammalian Cells. *J. Biol. Chem.* 2005, *280*, 4609−4616.

(5) Davies, T. H.; Ning, Y.-M.; Sanchez, E. R. Differential control of glucocorticoid receptor hormone-binding function by tetratricopeptide repeat (TPR) proteins and the immunosuppressive ligand FK506. *Biochemistry* 2005, *44*, 2030−2038.

(6) Periyasamy, S.; Hinds, T., Jr.; Shemshedini, L.; Shou, W.; Sanchez, E. R. FKBP51 and Cyp40 are positive regulators of androgen-dependent prostate cancer cell growth and the targets of FK506 and cyclosporin A. *Oncogene* 2010, *29*, 1691−1701.

(7) Ni, L.; Yang, C. S.; Gioeli, D.; Frierson, H.; Toft, D. O.; et al. FKBP51 promotes assembly of the Hsp90 chaperone complex and regulates androgen receptor signaling in prostate cancer cells. *Mol. Cell. Biol.* 2010, *30*, 1243−1253.

(8) Binder, E. B. The role of FKBP5, a co-chaperone of the glucocorticoid receptor in the pathogenesis and therapy of affective and anxiety disorders. *Psychoneuroendocrinology* 2009, *34*, S186−S195.

(9) Attwood, B. K.; Bourgognon, J. M.; Patel, S.; Mucha, M.; Schiavon, E.; et al. Neuropsin cleaves EphB2 in the amygdala to control anxiety. *Nature* **2011**, *473*, 372−375.

(10) Hartmann, J.; Wagner, K. V.; Liebl, C.; Scharf, S. H.; Wang, X. D.; et al. The involvement of FK506-binding protein 51 (FKBP5) in the behavioral and neuroendocrine effects of chronic social defeat stress. *Neuropharmacology* **2012**, *62*, 332−339.

(11) Touma, C.; Gassen, N. C.; Herrmann, L.; Cheung-Flynn, J.; Bull, D. R.; et al. FK506 Binding Protein 5 Shapes Stress Responsiveness: Modulation of Neuroendocrine Reactivity and Coping Behavior. *Biol. Psychiatry* **2011**, *70*, 928−936.

(12) O'Leary, J. C., 3rd; Dharia, S.; Blair, L. J.; Brady, S.; Johnson, A. G.; et al. A New Anti-Depressive Strategy for the Elderly: Ablation of FKBP5/FKBP51. *PLoS One* **2011**, *6*, e24840.

(13) Babine, R. E.; Villafranca, J. E.; Gold, B. G. FKBP immunophilin patents for neurological disorders. *Expert Opin Ther. Patents* **2005**, *15*, 555−573.

(14) Wang, X. J.; Etzkorn, F. A. Peptidyl-prolyl isomerase inhibitors. *Biopolymers* **2006**, *84*, 125−146.

(15) Keenan, T.; Yaeger, D. R.; Courage, N. L.; Rollins, C. T.; Pavone, M. E.; et al. Synthesis and activity of bivalent FKBP12 ligands for the regulated dimerization of proteins. *Bioorg. Med. Chem.* **1998**, *6*, 1309−1335.

(16) Holt, D. A.; Luengo, J. I.; Yamashita, D. S.; Oh, H. J.; Konilian, A. L.; et al. Design, synthesis, and kinetic evaluation of high-affinity FKBP ligands and the X-ray crystal structures of their complexes with FKBP 12. *J. Am. Chem. Soc.* **1993**, *115*, 9925−9938.

(17) Kozany, C.; Marz, A.; Kress, C.; Hausch, F. Fluorescent probes to characterise FK506-binding proteins. *ChemBioChem* **2009**, *10*, 1402−1410.

(18) Bracher, A.; Kozany, C.; Thost, A. K.; Hausch, F. Structural characterization of the PPIase domain of FKBP51, a cochaperone of human Hsp90. *Acta Crystallogr., Sect. D: Biol. Crystallogr.* **2011**, *67*, 549−559.

(19) Paulini, R.; Muller, K.; Diederich, F. Orthogonal multipolar interactions in structural chemistry and biology. *Angew. Chem., Int. Ed. Engl.* **2005**, *44*, 1788−1805.

(20) Birge, R. B.; Wadsworth, S.; Akakura, R.; Abeysinghe, H.; Kanojia, R.; et al. A role for schwann cells in the neuroregenerative effects of a non-immunosuppressive fk506 derivative, jnj460. *Neuroscience* **2004**, *124*, 351−366.

(21) Bull, D. J.; Maguire, R. J.; Palmer, M. J.; Wythes, M. J. Heterocyclic compounds as inhibitors of rotamase enzymes. WO/1999/045006, 1999.

(22) Varray, S.; Gauzy, C.; Lamaty, F.; Lazaro, R.; Martinez, J. Synthesis of cyclic amino acid derivatives via ring closing metathesis on a poly(ethylene glycol) supported substrate. *J. Org. Chem.* **2000**, *65*, 6787−6790.

(23) Stivanello, M.; Leoni, L.; Bortolaso, R. Synthesis of 1,5-bis(triphenylphosphonium)pentan-3-ol dichloride and its application to the preparation of 1,7-di(pyridin-3-yl)heptan-4-ol. *Org. Process Res. Dev.* **2002**, *6*, 807−810.

(24) Steiner, J. P.; Hamilton, G. S.; Ross, D. T.; Valentine, H. L.; Guo, H.; et al. Neurotrophic immunophilin ligands stimulate structural and functional recovery in neurodegenerative animal models. *Proc. Natl. Acad. Sci. U.S.A.* **1997**, *94*, 2019−2024.

(25) Riggs, D. L.; Cox, M. B.; Tardif, H. L.; Hessling, M.; Buchner, J.; et al. Noncatalytic role of the FKBP52 peptidyl-prolyl isomerase domain in the regulation of steroid hormone signaling. *Mol. Cell. Biol.* **2007**, *27*, 8658−8669.

(26) Wilson, K. P.; Yamashita, M. M.; Sintchak, M. D.; Rotstein, S. H.; Murcko, M. A.; et al. Comparative X-ray structures of the major binding protein for the immunosuppressant FK506 (tacrolimus) in unliganded form and in complex with FK506 and rapamycin. *Acta Crystallogr., Sect. D: Biol. Crystallogr.* **1995**, *51*, 511−521.

(27) Teague, S. J.; Stocks, M. J. The Affinity of the Excised Binding Domain of Fk-506 for the Immunophilin Fkbp12. *Bioorg. Med. Chem. Lett.* **1993**, *3*, 1947−1950.

(28) Birkenshaw, T. N.; Caffrey, M. V.; Cladingboel, D. E.; Cooper, M. E.; Donald, D. K.; et al. Synthetic Fkbp12 Ligands - Design and Synthesis of Pyranose Replacements. *Bioorg. Med. Chem. Lett.* **1994**, *4*, 2501−2506.

(29) Caffrey, M. V.; Cladingboel, D. E.; Cooper, M. E.; Donald, D. K.; Furber, M.; et al. Synthesis and Evaluation of Dual Domain Macrocyclic Fkbp12 Ligands. *Bioorg. Med. Chem. Lett.* **1994**, *4*, 2507−2510.

(30) Mase, N.; Inoue, A.; Nishio, M.; Takabe, K. Organocatalytic alpha-hydroxymethylation of cyclopentanone with aqueous formaldehyde: easy access to chiral delta-lactones. *Bioorg. Med. Chem. Lett.* **2009**, *19*, 3955−3958.

(31) Chen, A. Q.; Xu, J.; Chiang, W.; Chai, C. L. L-Threonine-catalysed asymmetric alpha-hydroxymethylation of cyclohexanone: application to the synthesis of pharmaceutical compounds and natural products. *Tetrahedron* **2010**, *66*, 1489−1495.

(32) Kim do, H.; Kim, K.; Chung, Y. K. A facile synthesis of the basic steroidal skeleton using a Pauson-Khand reaction as a key step. *J. Org. Chem.* **2006**, *71*, 8264−8267.

(33) Crabbe, P.; Dollat, J.-M.; Gallina, J.; Luche, J.-L.; Velarde, E.; et al. Steric course of cross coupling of organocopper reagents with allylic acetates. *J. Chem. Soc., Perkin Trans. 1* **1978**, 730−734.

(34) Leibrock, B.; Vostrowsky, O.; Hirsch, A. Synthesis of new cyclic homoconjugated oligodiacetylenes. *Eur. J. Org. Chem.* **2001**, 4401−4409.

(35) Tatlock, J. H.; Kalish, V. J.; Parge, H. E.; Knighton, D. R.; Showalter, R. E.; et al. High-affinity FKBP-12 ligands derived from (R)-(-)-carvone. Synthesis and evaluation of FK506 pyranose ring replacements. *Bioorg. Med. Chem. Lett.* **1995**, *5*, 2489−2494.

(36) Wu, Y. L.; Li, L. S. An efficient method for synthesis of alpha-keto acid esters from terminal alkynes. *Tetrahedron Lett.* **2002**, *43*, 2427−2430.

(37) Liu, K. G.; Yan, S.; Wu, Y. L.; Yao, Z. J. A new synthesis of Neu5Ac from D-glucono-delta-lactone. *J. Org. Chem.* **2002**, *67*, 6758−6763.

(38) Tatlock, J. H. Oxidation of Alkynyl Ethers with Potassium-Permanganate - a New Acyl Anion Equivalent for the Preparation of Alpha-Keto Esters. *J. Org. Chem.* **1995**, *60*, 6221−6223.

(39) Armistead, M. D.; Harding, W. M.; Boger, S. J. Biologically active acylated amino acid derivatives. US6187784, 1998.

(40) Leslie, A. G. W. Recent changes to the MOSFLM package for processing film and image plate data. *Jnt CCP4/ESF-EACMB Newsl. Protein Crystallogr.* **1992**, 26.

(41) Kabsch, W. Xds. *Acta Crystallogr., Sect. D: Biol. Crystallogr.* **2010**, *66*, 125−132.

(42) Evans, P. R. SCALA. *Jnt CCP4/ESF-EACMB Newsl. Protein Crystallogr.* **1997**, *33*, 22−24.

(43) French, S.; Wilson, K. Treatment of Negative Intensity Observations. *Acta Crystallogr., Sect. A* **1978**, *34*, 517−525.

(44) Vagin, A.; Teplyakov, A. Molecular replacement with MOLREP. *Acta Crystallogr., Sect. D: Biol. Crystallogr.* **2010**, *66*, 22−25.

(45) Schuttelkopf, A. W.; van Aalten, D. M. F. PRODRG: a tool for high-throughput crystallography of protein-ligand complexes. *Acta Crystallogr., Sect. D: Biol. Crystallogr.* **2004**, *60*, 1355−1363.

(46) Murshudov, G. N.; Skubak, P.; Lebedev, A. A.; Pannu, N. S.; Steiner, R. A.; et al. REFMAC5 for the refinement of macromolecular crystal structures. *Acta Crystallogr., Sect. D: Biol. Crystallogr.* **2011**, *67*, 355−367.

(47) Emsley, P.; Lohkamp, B.; Scott, W. G.; Cowtan, K. Features and development of Coot. *Acta Crystallogr., Sect. D: Biol. Crystallogr.* **2010**, *66*, 486−501.

(48) Gopalakrishnan, R.; Kozany, C.; Wang, Y.; Schneider, S.; Hoogeland, B.; Bracher, A.; Hausch, F. Exploration of Pipecolate Sulfonamides as Binders of the FK506-Binding Proteins 51 and 52. *J. Med. Chem.* **2012**, DOI: 10.1021/jm201747c.

(49) Schmidt, M. V.; Paez-Pereda, P.; Holsboer, F.; Hausch, F. The Prospect of FKBP51 as a Drug Target. *ChemMedChem* **2012**, DOI: 10.1002/cmdc.201200137.